

Method development and analysis of the water content of the maximally freeze concentrated solution suitable for protein lyophilisation

Original

Method development and analysis of the water content of the maximally freeze concentrated solution suitable for protein lyophilisation / Seifert, Ivonne; Bregolin, Alessandro; Fissore, Davide; Friess, Wolfgang. - In: EUROPEAN JOURNAL OF PHARMACEUTICS AND BIOPHARMACEUTICS. - ISSN 0939-6411. - STAMPA. - 153:(2020), pp. 36-42.
[10.1016/j.ejpb.2020.05.027]

Availability:

This version is available at: 11583/2829412 since: 2020-06-15T11:14:52Z

Publisher:

Elsevier

Published

DOI:10.1016/j.ejpb.2020.05.027

Terms of use:

This article is made available under terms and conditions as specified in the corresponding bibliographic description in the repository

Publisher copyright

Elsevier postprint/Author's Accepted Manuscript

© 2020. This manuscript version is made available under the CC-BY-NC-ND 4.0 license
<http://creativecommons.org/licenses/by-nc-nd/4.0/>. The final authenticated version is available online at:
<http://dx.doi.org/10.1016/j.ejpb.2020.05.027>

(Article begins on next page)

Method Development and Analysis of the Water Content of the Maximally Freeze Concentrated Solution Suitable for Protein Lyophilisation

Ivonne Seifert¹, Alessandro Bregolin², Davide Fissore², Wolfgang Friess¹

¹Department of Pharmacy, Pharmaceutical Technology and Biopharmaceutics, Ludwig-Maximilians-Universität München, Munich, Germany

²Department of Applied Science and Technology, Politecnico di Torino, Torino, Italy

Abstract

During freeze-drying of a liquid formulation, a freeze-concentrate is formed in the first phase, the freezing step. Understanding the composition of the maximally freeze concentrated solution can help to judge the process stability of biopharmaceuticals during lyophilisation. Our objective was to develop a suitable method to determine the water content of the maximally freeze concentrated solution using differential scanning calorimetry (DSC). Three different methods were compared: (i) the intercept of the glass transition temperature of the maximally freeze concentrated solution T_g' and the melting temperature T_m for a concentration series, (ii) the linear regression of the melting enthalpy starting from the onset of T_g' until the end of the melting event for a concentration series, and (iii) a one-point determination of the amount of unfrozen water. While Method 1 is accurate but requires the analysis of a high number of samples, Method 3 requires only one single sample, with a loss of accuracy. Method 2 works best taking sample preparation and accuracy into account. Various systems

containing sugar (sucrose, trehalose) and other excipients (histidine buffer, phosphate buffer, sodium chloride, arginine hydrochloride, arginine citrate) were evaluated with different antibody concentrations to evaluate the composition of the maximally freeze concentrated solution. The freeze concentrates exhibited a water content of 20 - 30%, slightly dependent on the excipients, but independent of the antibody concentration. The methodology we developed is broadly applicable for the analysis of the composition of maximally freeze concentrated solutions and can help to elucidate protein stability during lyophilisation.

1. Introduction

Cooling of aqueous solutions below the freezing temperature leads to formation of ice. The crystallisation of ice corresponds to a removal of water from the system and an up-concentration of all solutes remaining in the unfrozen phase. This process is known as freeze concentration. During freeze drying of biological material or biopharmaceuticals, freeze concentration affects the behaviour of the proteins through solute concentration, potential crystallisation of buffer components accompanied by a pH shift, phase separation, increased viscosity, increased ionic strength, or interfacial stress [1-7]. An increased viscosity during freezing can lead for example to phase separation with a protein-rich phase, potentially lacking stabilising excipients [2, 4, 8]. On the other hand, reaction rates can be reduced with increased viscosity [9, 10]. A pH shift through buffer component crystallisation and increased ionic strength can change the protein-protein interactions [11, 12]. Additionally, freeze concentration is accompanied with both thermodynamic and kinetic changes causing either stabilisation or destabilisation of a protein. It also need to be kept in mind that since freeze concentration continues until ice formation is complete and that therefore protein perturbation occurs over a longer time frame [13].

The freeze concentrated solution is defined by the mass fraction of solids w_g' and the mass fraction of unfrozen water w_{uf} [14]. w_{uf} and w_g' can be determined by techniques such as cryoscopy and differential scanning calorimetry (DSC). Another approach is to follow the phase change state via the product temperature during ice nucleation within the freeze drying itself [14-20].

Different methods are described in literature to calculate w_g' using DSC. One approach is to measure a single sample. The amount of frozen water in the sample can be calculated from the ice melting endotherm by taking reference to the ice melting endotherm of pure water. Finally, w_g' can be obtained based on the total solid content of the solution via the amount of unfrozen water [21, 22]. Typically, the melting enthalpy of pure water is compared with the melting enthalpy of a 20% w/w solution. For sucrose, trehalose, and glycerol w_g' can be 64%, 83%, and 54%, respectively [21]. A w_g' of 68% for glycerol results if using a stepwise evaluation of the apparent melting heat and calculating the ice fraction. Thereby, the sample temperature is alternated in a series of heating and isothermal steps [23]. Different w_g' values for different solid contents are observed for this type of one point determination [24]. Since ice vitrification might not be completed after a simple freezing step, annealing should be applied. By this a higher sucrose w_g' of 81% (w/w) is obtained [25].

In contrast to a one point determination method, two approaches using intercepts of fits are possible to determine w_g' based on a concentration dependent phase diagram (Figure 1). Literature is divided over the glass transition temperature of the maximally freeze concentrated solution, stating two transitions as T_g' and T_g'' . The Gordon-Taylor equation can be used to fit exemplarily the glass transition of sucrose-water mixtures at different ratios. The intercept of the T_g curve as a function of sucrose concentration and T_g'' at approx. -45°C for sucrose renders w_g' . Alternatively, the intercept of the melting temperature (T_m) as a function of sucrose concentration curve and T_g' at approx. -34°C for sucrose leads to w_g' . For sucrose a w_g' of 81 - 83% (w/w) results with both methods [26-31]. For trehalose different w_g' values, ranging from 70% to 83% (w/w), are reported [32, 33].

Furthermore, a linear function of the ice melting enthalpy against the solid concentration can be extrapolated to $\Delta H = 0 \text{ J/g}$ to obtain w_g' [34-36]. This is a simple method without the need for major mathematical theories. Thereby, a w_g' of sucrose of 79% (w/w) results [34]. Thus, overall rather different w_g' values are reported for sucrose ranging from 64% [21, 37], 77% [29], up to 82% [25, 26, 38] and for trehalose ranging from 71 to 83% [32, 33]. Other reported w_g' values of excipients relevant

for freeze-drying are 46% for polyethylene glycol 40000, which increased with the addition of sucrose at a 1:1 ratio to 60% [39], and 81% (w/w) for citric acid [40].

w_g' is currently not considered, when it comes to freeze drying of proteins. Knowing the exact composition can help to prepare the freeze concentrates and study e.g. protein-protein interactions or protein stability excluding ice-freeze concentrate interface effects. To answer these questions and due to the substantial deviation of w_g' values stated in literature, the aim of this study was to evaluate and compare three different DSC based approaches to determine w_g' of sucrose as model substance: (i) using the intercept of the T_g' and T_m curves; (ii) using a linear regression of the melting endotherm; and (iii) using a one point measurement of the frozen water based on the melting endotherm. The methods were to be evaluated with respect to accuracy and effort. Subsequently the w_g' of different formulations relevant for lyophilisates of biopharmaceuticals was to be analysed. Besides sugar and protein also buffers, amino acids, and NaCl as excipients were evaluated.

2. Materials and Methods

2.1 Materials

Sucrose, L-histidine base, L-histidine monohydrochloride, L-arginine base, and L-arginine hydrochloride monohydrate (ArgHCl) were purchased from Sigma-Aldrich Chemie GmbH, Steinheim, Germany. Sodium dihydrogen phosphate dihydrate, disodium hydrogen phosphate dihydrate, citric acid anhydrous, and sodium chloride were obtained from VWR International, Ismaning, Germany. All samples were prepared with highly purified water (HPW; Sartorius Arium Pro, Sartorius, Göttingen, Germany). A monoclonal IgG₁ antibody (mAb) in 15 mM histidine buffer pH 5.3 was used as standard protein.

2.2 Methods

2.2.1 Determination of w_g'

2.2.1.1 Differential scanning calorimetry (DSC)

T_g' and T_m were determined with a Netzsch Polyma 214 (Netzsch, Selb, Germany), a DSC 821^e (Mettler Toledo, Gießen, Germany), a TA Discovery (TA Instruments, New Castle, DE, USA), and a TA Q2000 (TA Instruments) under N₂ atmosphere. Low concentration samples are difficult to determine due to a high requirement for sensitivity and therefore different instruments were explored. 15 - 25 μ L solution with 0% up to 65% (w/w) solid content was weighted into aluminium crucibles and sealed hermetically. The samples were cooled from 20°C to -60°C (-40°C only for Netzsch) at 5°C/min, reheated to -30°C at 2°C/min, held for 1 h to ensure complete ice formation [29], cooled to -60°C (-40°C only for Netzsch) at 5°C/min, and finally heated to 20°C at 2°C/min. Calibration was performed with indium as provided by the manufacturer. Netzsch Proteus Analysis, Mettler STAR^e, TRIOS, and TA Universal Analysis software were used for data analysis. The specific heat capacity of water (ΔC_p) was evaluated with a tangential step before and after the ice melting in a pure HPW sample. The melting enthalpy (ΔH) was evaluated by an integration starting from the beginning of the T_g' endothermic shift and ending at the return to baseline after the melting event. Sigmoidal or spline baseline settings were used for the integration.

2.2.1.2 Calculation of w_g'

2.2.1.2.1 Method 1: Intercept of T_g' and T_m curves

Values of T_m vs. the relative solid content (x) were fitted to the Chen model (Equation (1)), an extension of the Clausius-Clapeyron equation [31] with T_m and T_w being the melting temperature of sample and HPW, respectively, β the molar freezing temperature constant for water (1860 kg·K/mol), M the molar mass of water. B and E were fitted to the experimental data with OriginPro 2018. The onset temperature of T_g' was fitted as horizontal line. w_g' was determined as the intercept of the T_m curve and the onset temperature of T_g' line.

Equation (1)

$$T_m = T_w + \frac{\beta}{M} \cdot \ln \frac{1 - x - Bx}{1 - x - Bx + Ex}$$

2.2.1.2.2 Method 2: Linear regression

The obtained DSC thermograms were integrated from the onset temperature of T_g' until the end of the melting peak with a sigmoidal baseline type to obtain the melting enthalpy ΔH . A linear regression function of the ice melting enthalpy against the solid concentration was extrapolated to $\Delta H = 0$ J/g to calculate w_g' .

2.2.1.2.3 Method 3: Single sample determination

The effective fusion enthalpy of ice in solution L_e was calculated from the specific heat coefficient ΔC_p , T_m and T_w (Equation (2)). The amount of frozen water w_f (Equation (3)) is obtained from the melting enthalpy of the sample ΔH_s , the sample mass m_s filled in the pan, the melting enthalpy of water ΔH_w and L_e (adapted from [24] including the assumptions of neglectable effects of the ice melting enthalpy on the temperature and heat dilution). Finally, w_g' is calculated sample dependent with the solid content (solute concentration c_s and sample mass m_s), the total water content w_{total} and w_f (Equation (4)).

Equation (2)

$$L_e = \Delta C_p \cdot (T_m - T_w)$$

Equation (3)

$$w_f = \frac{\Delta H_s \cdot m_s}{\Delta H_w + L_e}$$

$$w_g' = \frac{c_s \cdot m_s}{(W_{total} - W_f) + c_s \cdot m_s}$$

2.2.2 Determination of w_g' in ternary and higher systems

The compositions tested are listed in Table 1. Arginine citrate (ArgCitr) powder (residual moisture 5.35%) was produced by spray drying (Mini Spray Dryer B-290, Buchi, Essen, Germany) an arginine citrate solution pH 6.0. An 8% (w/w) solution was spray dried at 140°C inlet temperature, 81°C outlet temperature, 70% aspiration, 600 L flow, and 10% pump speed. mAb was dialysed against the individual buffers or HPW with a 10-fold buffer exchange in Vivaspin® 20 Ultrafiltration Uni (30 kDa, Sartorius, Goettingen, Germany) and upconcentrated if necessary.

The formulations were prepared at consistent solute ratios but different total solid content ranging from 10% up to 50% w/w.

3. Results and Discussion

3.1 Evaluation of methods to determine a maximally freeze concentrated system

The first aim of this study was to identify the most suitable method to determine w_g' of a maximally freeze concentrated system balancing accuracy and sample and time consumption. 1.5% up to 65% (w/w) sucrose solutions were analysed using three methods.

The first method makes use of the intercept of two curves. The first curve represents the linear fit of the onset of T_g' . The second curve reflecting the T_m peak is fitted with the Chen model, adapted from the Clausius-Clapeyron equation [31, 41] resulting in B and E of 0.056 ± 0.0063 and $8.19 \cdot 10^{-5} \pm 9.84 \cdot 10^{-6}$, respectively. The T_m curve and T_g' onset temperature (around -34°C) complies with literature data [42, 43]. The intercept of the two curves reflects w_g' (Figure 2). Method 1 results in $77.4 \pm 1.7\%$ sucrose in the maximally freeze concentrated system.

Method 2 utilises the solute concentration dependent change in the melting enthalpy to obtain w_g' . The DSC thermogram is integrated for ΔH starting at the onset of T_g' until the end of the melting event (Figure 3). The linear fit of ΔH is extrapolated to 0 J/g, which reflects the freeze concentrated state (Figure 4) [35]. This method 2 results in a w_g' of $75.2 \pm 0.8\%$ sucrose in this binary freeze concentrate.

The third method directly calculates w_g' (Figure 5B) from the amount of frozen water of a specific sample obtained from the DSC melting enthalpy (Figure 5A). The experimental ΔC_p of 2.10 ± 0.01 J/gK, T_w of $0.4 \pm 0.3^\circ\text{C}$, and ΔH_w of 347 ± 2 J/g are in agreement with the literature values of 2.06 J/gK, 0°C , and 333 J/g, respectively [44, 45]. An exemplary thermogram can be found in supplementary information. This method results in w_g' for sucrose of 77.0% in the freeze concentrated state. The frozen water content could be determined with low standard deviation independent of the sugar concentration. But the small error in the amount of unfrozen water at low concentration samples led to high standard deviations in the calculated w_g' . Sugar concentrations of 30% and higher prompted reliable w_g' values with a low standard deviation. Thus, 3.5% (w/w) sucrose resulted in a w_g' of $79.3 \pm 10.6\%$, whereas 62% (w/w) sucrose showed a w_g' of $77.7\% \pm 0.2\%$. But these high solid contents are not used in lyophilisation of parenteral products.

All three tested methods resulted in a narrow range of w_g' values of 75.4 – 77.4%, whereas literature stated w_g' values between 64% and 83% [21, 25, 27, 29, 34]. Comparing the three methods, the first method is the most accurate since it requires only the evaluation of temperatures without integration of thermograms. However, a rather high number of samples with high solid content needs to be prepared and analysed, which is time consuming. This is mandatory to apply the Chen model to fit T_m and a new fit is required for each formulation. Considering poorly soluble excipients or rather high concentrations of proteins like antibodies, this method has its limitations. The second method could be used with less, at least five different concentrations preferably between 5% and 45%, for a simple linear fit of the melting enthalpy (same result for w_g' with $p < 0.05$ according to t-test). The third method is an even further simplification using only one single sample with a solid content of 30% or higher. With lower solid content, the error becomes unacceptable. Analysis of only one higher

concentration sample showed more reliable results but still differed from the mean. DSC systems with higher sensitivity might be used with lower solid contents rendering method 3 superior. Overall, method 2 is the most applicable approach taking sample number and therefore measurement time, calculation of w_g' , and reliability of the results into account. Method 2 was therefore subsequently used to analyse the w_g' of different formulations.

3.2 W_g' in protein containing samples

Subsequently method 2 was used to evaluate w_g' of sucrose and trehalose based formulations. The effect of histidine buffer and phosphate buffer at pH 5.3 and 7.4 as well NaCl was tested. In addition, the influence of the mAb concentration on the composition of the freeze concentrate was studied considering up to 200 g/L protein formulations. Furthermore, sugar free systems based on arginine hydrochloride, arginine citrate, and sodium chloride as sole excipient were tested with and without mAb.

Adding mAb to sucrose at different ratios up to Suc:mAb 7:20 did not impact w_g' , with values between 74.3% and 78.0% for different mAb concentrations and $75.2 \pm 0.8\%$ for pure sucrose. mAb addition did not lead to a change in w_g' of the system (Figure 6). In addition, we could show that buffer did not significantly lower w_g' of Suc + His 5.3 (w_g' of $73.1 \pm 1.6\%$), Suc + His 7.4 ($73.8 \pm 1.4\%$), Suc + Phos 5.3 ($72.9 \pm 1.2\%$), and Suc + Phos 7.4 ($73.6 \pm 1.5\%$). Addition of salt resulted in a decrease of w_g' of freeze concentrates to $72.4 \pm 2.3\%$ and $70.4 \pm 2.0\%$ for Suc + 0.4 NaCl and Suc + 0.8 NaCl as found by Her et al. [46]. NaCl alone without further excipient with mAb crystallised during the freezing and annealing process in the DSC. The eutectic concentration of NaCl-water is composed of 23.3% (w/w) NaCl [47]. Therefore, the integration was performed starting at the beginning of the eutectic temperature until the end of the melting event. W_g' of crystallised NaCl and mAb at a 0.4:1 ratio was $67.7 \pm 3.4\%$, which was significant lower compared to the system Suc + 0.4 NaCl containing sucrose:NaCl:mAb in a ratio of 7:0.4:1 ($p < 0.05$, t-test).

Trehalose as alternative disaccharide rendered a w_g' similar to sucrose with $73.0 \pm 2.7\%$. Crystallisation of trehalose can occur in case of annealing and thereby influencing w_g' [48]. DSC thermograms did not indicate crystallisation. Again, the addition of histidine buffer pH 5.3 to the sugar did not affect w_g' .

Sugar-free formulations based on L-arginine may present an alternative for freeze-drying of protein drugs [49]. Other than sugar, arginine does not promote preferential exclusion in the solution to be freeze dried. Arginine is able to form hydrogen bonds with protein molecules and undergoes ion-dipole interactions [50], which might affect w_g' . Arginine hydrochloride can reduce protein-protein interactions, which can lead to a significant reduction in viscosity at high concentrations [51]. Such high concentrations are expected for protein containing freeze-concentrates. ArgCitr, ArgHCl, and ArgHCl with mAb (ArgHCl:mAb 5:0.2) showed w_g' values of $79.6 \pm 3.1\%$, $72.4 \pm 2.0\%$ and $72.7 \pm 2.3\%$, respectively. Due to the T_g' and T_g increasing influence of citric acid, w_g' of ArgCitr might be influenced [52].

Subsequently the w_g' of the mAb and its potential effect in mixtures with excipients was analysed. However, w_g' is difficult to determine since a glass transition of the mAb cannot be detected. It is estimated to be at around -15°C [53]. According to the onset of the melting peak in the thermograms (drop in baseline) the onset temperature of T_g' could be approximated to be around -25°C ranging from 0.2% mAb up to 30% mAb (Figure 7). The obtained w_g' of pure mAb was $80.8 \pm 3.4\%$.

With the determined w_g' values, the composition of the maximally freeze concentrate can be calculated taking the initial solid content of the formulation into account. Other than the solid content at the concentration of w_g' only unfrozen water remains. The w_g' of mAb-sugar mixtures was independent of the mAb concentration. However, increasing the mAb concentration results in different mAb to sugar or excipient ratios in the freeze concentrate. Table 2 states some examples with different mAb to sucrose ratios, ranging from low to high mAb concentrations. A formulation with 20% mAb will result in around 56% (w/w) mAb in the concentrated state with only 22% (w/w) H_2O and 20% (w/w) sucrose.

Histidine buffer resulted in a marked decrease in ionic strength of 275 mM to 156 mM with increasing pH values. Phosphate buffer increased in ionic strength to 302 mM and 391 mM for a pH of 5.3 and 7.4, respectively. NaCl caused an enormous increase in ionic strength in the freeze concentrated to 1.4 M. The high ionic strength in NaCl-containing samples could possibly influence the system by decreasing T_g' and thus w_g' [14]. However, w_g' was influenced neither by different sugar concentrations, differences in ionic strength nor the mAb concentration. No systematic analysis of w_g' with different mAb containing formulations has been stated so far. The up-concentration of proteins can lead to an increase in attractive protein-protein interactions or phase separation with a loss in stabilising protein-excipient interactions. These effects in combination with high ionic strength could foster potential protein instability [4, 7].

Furthermore, the freeze concentrate was also determined to be between 72.4% and 79.6% in sugar free arginine systems. Crystallisation of NaCl as sole excipient resulted in slightly lower total solid content with around 67.6% in the up-concentrated state, which was significant lower compared to amorphous matrix forming systems.

4. Conclusion

Different DSC methods were previously reported in literature to determine the amount and the water content of the maximally freeze concentrated solution formed upon freezing solutions [24, 31, 35]. Knowledge of the composition can help to judge protein drug instability during freeze-drying and can enable to prepare the freeze concentrate and analyse its properties. We evaluated three different approaches for analysis of the freeze concentrate composition. Using the intercept of concentration dependent T_g' and T_m curves requires a large number of samples with different total solid content and samples of high total solid content of >30%. The high number of different samples results in an accurate result for the composition of the freeze concentrate. Analysis of the frozen water content and with that w_g' of only one sample is rather limited and dependent on the total solid content and the sensitivity of the DSC system. Higher solid contents are recommended for this method. A very good

compromise is to determine the frozen water content of samples of 10 – 30% solid content based on the AUC of the melting event and to extrapolate. This method renders reproducible results with little sample and time consumption.

Overall, the total solid content w_g' of the maximally freeze concentrated solution of sugar based amorphous protein solutions lays between 70% and 80% total, regardless the different additional excipients. Buffers or salt tend to decrease the w_g' values, however, without statistical significance. The mAb concentrations did not affect w_g' . Sugar free arginine formulations show similar w_g' values between 70% and 80%.

The process of freeze concentration leads to increased viscosities, potential crystallisation of solutes, phase separation, or high ionic strengths [2, 4, 7]. Thereby, increased protein concentration is accompanied by more protein-protein interactions. Eventually, the combination with pH shifts due to buffer crystallisation or high ionic strength can force protein instabilities. In following studies, freeze concentrates of different formulations will be produced and protein stability evaluated accordingly.

Acknowledgement

We would like to thank David Thomas from Vectura Group Plc., Wenqi Wu from the University of Copenhagen, and Robert Cornell from the University of Cambridge for the opportunity to use their DSC equipment and expertise. Special thanks go to Bakul Bhatnagar from Pfizer for sharing his helpful hints and tricks about DSC measurements with us.

References

1. Pincock, R.E., *Reactions in frozen systems*. Acc Chem Res, 1969. 2(4): p. 97-103.
2. Heller, M.C., J.F. Carpenter, and T.W. Randolph, *Effects of phase separating systems on lyophilized hemoglobin*. J Pharm Sci, 1996. 85(12): p. 1358-1362.
3. Heller, M.C., J.F. Carpenter, and T.W. Randolph, *Conformational stability of lyophilized PEGylated proteins in a phase-separating system*. J Pharm Sci, 1999. 88(1): p. 58-64.
4. Randolph, T.W., *Phase separation of excipients during lyophilization: Effects on protein stability*. J Pharm Sci, 1997. 86(11): p. 1198-1203.

5. Izutsu, K.-I. and S. Kojima, *Freeze-Concentration Separates Proteins and Polymer Excipients Into Different Amorphous Phases*. Pharm Res, 2000. 17(10): p. 1316-1322.
6. Gómez, G., M.J. Pikal, and N. Rodríguez-Hornedo, *Effect of Initial Buffer Composition on pH Changes During Far-From-Equilibrium Freezing of Sodium Phosphate Buffer Solutions*. Pharm Res, 2001. 18(1): p. 90-97.
7. Pikal, M.J., *Mechanisms of Protein Stabilization during Freeze-Drying and Storage*, in *Freeze-Drying/Lyophilization Of Pharmaceutical & Biological Products, Third Edition*. 2004, Informa Healthcare.
8. Heller, M.C., J.F. Carpenter, and T.W. Randolph, *Manipulation of lyophilization-induced phase separation: implications for pharmaceutical proteins*. Biotechnol Prog, 1997. 13(5): p. 590-596.
9. van de Weert, M. and T.W. Randolph, *Physical Instability of Peptides and Proteins*, in *Pharmaceutical Formulation Development of Peptides and Proteins*, L. Hovgaard, S. Frokjaer, and M. van de Weert, Editors. 2013, CRC Press Taylor & Francis Group: London.
10. Hagen, S.J., J. Hofrichter, and W.A. Eaton, *Protein reaction kinetics in a room-temperature glass*. Science, 1995. 269(5226): p. 959-962.
11. Kolhe, P., E. Amend, and S.K. Singh, *Impact of freezing on pH of buffered solutions and consequences for monoclonal antibody aggregation*. Biotechnol Prog, 2010. 26(3): p. 727-733.
12. Zbacnik, T.J., et al., *Role of Buffers in Protein Formulations*. J Pharm Sci, 2017. 106(3): p. 713-733.
13. Bhatnagar, B.S., R.H. Bogner, and M.J. Pikal, *Protein Stability During Freezing: Separation of Stresses and Mechanisms of Protein Stabilization*. Pharm Dev Technol, 2007. 12(5): p. 505-523.
14. Xu, M., et al., *Study on the Unfrozen Water Quantity of Maximally Freeze-Concentrated Solutions for Multicomponent Lyoprotectants*. J Pharm Sci, 2017. 106(1): p. 83-91.
15. Woods, E.J., et al., *Equations for obtaining melting points for the ternary system ethylene glycol/sodium chloride/water and their application to cryopreservation*. Cryobiology, 1999. 38(4): p. 403-407.
16. Shepard, M.L., C.S. Goldston, and F.H. Cocks, *The H₂O-NaCl-glycerol phase diagram and its application in cryobiology*. Cryobiology, 1976. 13(1): p. 9-23.
17. Ross, H.K., *Cryoscopic Studies - Concentrated Solutions of Hydroxy Compounds*". Ind Eng Chem, 1954. 46(3): p. 601-610.
18. Arvanitoyannis, I., et al., *Calorimetric study of the glass transition occurring in aqueous glucose: Fructose solutions*. J Sci Food Agric, 1993. 63(2): p. 177-188.
19. Searles, J.A., J.F. Carpenter, and T.W. Randolph, *The ice nucleation temperature determines the primary drying rate of lyophilization for samples frozen on a temperature-controlled shelf*. J Pharm Sci, 2001. 90(7): p. 860-871.
20. Assegehegn, G., et al., *The Importance of Understanding the Freezing Step and its Impact on Freeze Drying Process Performance*. J Pharm Sci, 2018.
21. Levine, H. and L. Slade, *Thermomechanical properties of small-carbohydrate-water glasses and 'rubbers'. Kinetically metastable systems at sub-zero temperatures*. Journal of the Chemical Society, Faraday Transactions 1: Physical Chemistry in Condensed Phases, 1988. 84(8).
22. Levine, H. and L. Slade, *A polymer physico-chemical approach to the study of commercial starch hydrolysis products (SHPs)*. Carbohydr Polym, 1986. 6(3): p. 213-244.
23. Liesebach, J., M. Lim, and T. Rades, *Determination of unfrozen matrix concentrations at low temperatures using stepwise DSC*. Thermochim Acta, 2004. 411(1): p. 43-51.
24. Weng, L., C. Chen, and W. Li, *Calorimetric and molecular simulation study on unfrozen water characteristics in aqueous sugar solutions: implications for biopreservation*. Mol Simul, 2015. 41(9): p. 691-698.
25. Ablett, S., M.J. Izzard, and P.J. Lillford, *Differential scanning calorimetric study of frozen sucrose and glycerol solutions*. J Chem Soc, Faraday Trans, 1992. 88(6): p. 789-794.

26. Chang, L., et al., *Using modulated DSC to investigate the origin of multiple thermal transitions in frozen 10% sucrose solutions*. *Thermochim Acta*, 2006. 444(2): p. 141-147.
27. Liesebach, J., T. Rades, and M. Lim, *A new method for the determination of the unfrozen matrix concentration and the maximal freeze-concentration*. *Thermochim Acta*, 2003. 401(2): p. 159-168.
28. Miller, D.P., J.J. de Pablo, and H. Corti, *Thermophysical Properties of Trehalose and Its Concentrated Aqueous Solutions*. *Pharm Res*, 1997. 14(5): p. 578-590.
29. Roos, Y. and M. Karel, *Amorphous state and delayed ice formation in sucrose solutions*. *Int J Food Sci Tech*, 1991. 26(6): p. 553-566.
30. Roos, Y.H., *Frozen state transitions in relation to freeze drying*. *J Therm Anal*, 1997. 48(3): p. 535-544.
31. Ruiz-Cabrera, M.A., et al., *State diagrams for mixtures of low molecular weight carbohydrates*. *J Food Eng*, 2016. 171: p. 185-193.
32. Kawai, H., et al., *Hydration of oligosaccharides: Anomalous hydration ability of trehalose*. *Cryobiology*, 1992. 29(5): p. 599-606.
33. Slade, L. and H. Levine, *Non-equilibrium behavior of small carbohydrate-water systems*. *Pure Appl Chem*, 1988. 60(12): p. 1841-1864.
34. Schawe, J.E.K., *A quantitative DSC analysis of the metastable phase behavior of the sucrose-water system*. *Thermochim Acta*, 2006. 451(1-2): p. 115-125.
35. Rahman, M.S., *State Diagram of Date Flesh Using Differential Scanning Calorimetry (DSC)*. *Int J Food Prop*, 2004. 7(3): p. 407-428.
36. Ablett, S., *Modelling of Heat Capacity-Temperature Data for Sucrose-Water Systems*. *J CHEM SOC FARADAY TRANS*, 1992. 88(6): p. 795-802.
37. Goff, H.D., *Low-temperature stability and the glassy state in frozen foods*. *Food Res Int*, 1992. 25(4): p. 317-325.
38. Pikal, M.J., et al., *The nonsteady state modeling of freeze drying: in-process product temperature and moisture content mapping and pharmaceutical product quality applications*. *Pharm Dev Technol*, 2005. 10(1): p. 17-32.
39. Bhatnagar, B.S., et al., *Investigation of PEG crystallization in frozen PEG-sucrose-water solutions: II. Characterization of the equilibrium behavior during freeze-thawing*. *J Pharm Sci*, 2010. 99(11): p. 4510-4524.
40. Bogdan, A., M.J. Molina, and H. Tenhu, *Freezing and glass transitions upon cooling and warming and ice/freeze-concentration-solution morphology of emulsified aqueous citric acid*. *Eur J Pharm Biopharm*, 2016. 109: p. 49-60.
41. Sablani, S.S., R.M. Syamaladevi, and B.G. Swanson, *A Review of Methods, Data and Applications of State Diagrams of Food Systems*. *Food Engineering Reviews*, 2010. 2(3): p. 168-203.
42. Gülseren, İ. and J.N. Coupland, *Ultrasonic properties of partially frozen sucrose solutions*. *J Food Eng*, 2008. 89(3): p. 330-335.
43. Goff, H.D., E. Verespej, and D. Jermann, *Glass transitions in frozen sucrose solutions are influenced by solute inclusions within ice crystals*. *Thermochim Acta*, 2003. 399(1-2): p. 43-55.
44. Becker, B.R. and B.A. Fricke, *FREEZING | Principles*, in *Encyclopedia of Food Sciences and Nutrition (Second Edition)*, B. Caballero, Editor. 2003, Academic Press: Oxford. p. 2706-2711.
45. Widmann, G. and R. Riesen, *The glass transition of water and aqueous systems*. *J Therm Anal Calorim*, 1998. 52(1): p. 109-113.
46. Her, L.-M., M. Deras, and S.L. Nail, *Electrolyte-Induced Changes in Glass Transition Temperatures of Freeze-Concentrated Solutes*. *Pharm Res*, 1995. 12(5): p. 768-772.
47. Han, B., et al., *A quantitative analysis on latent heat of an aqueous binary mixture*. *Cryobiology*, 2006. 52(1): p. 146-151.
48. Sundaramurthi, P. and R. Suryanarayanan, *Trehalose Crystallization During Freeze-Drying: Implications On Lyoprotection*. *The Journal of Physical Chemistry Letters*, 2010. 1(2): p. 510-514.

49. Stärtzel, P., *Arginine as an Excipient for Protein Freeze-Drying: A Mini Review*. J Pharm Sci, 2018. 107(4): p. 960-967.
50. Arakawa, T., et al., *Biotechnology applications of amino acids in protein purification and formulations*. Amino Acids, 2007. 33(4): p. 587-605.
51. Tsumoto, K., et al., *Role of Arginine in Protein Refolding, Solubilization, and Purification*. Biotechnol Prog, 2004. 20(5): p. 1301-1308.
52. Izutsu, K.-I., et al., *Freeze-Drying of Proteins in Glass Solids Formed by Basic Amino Acids and Dicarboxylic Acids*. Chem Pharm Bull, 2009. 57(1): p. 43-48.
53. Pansare, S.K. and S.M. Patel, *Practical Considerations for Determination of Glass Transition Temperature of a Maximally Freeze Concentrated Solution*. AAPS PharmSciTech, 2016. 17(4): p. 805-819.

List of Tables

Table 1: Formulations used for DSC experiments to evaluate w_g' . The ratios of different excipients including sugar and buffer to mAb are stated in *italic*. The formulations were prepared at consistent solute ratios ranging from 10% up to 50% w/w solid content.

Table 2: Exemplary freeze concentrate compositions. Ratios of solids in starting liquid upconcentrated to the total solid content w_g' . H₂O in the concentrated state is synonymous with unfrozen water.

List of Figures

Figure 1: Schematic phase diagram, adapted from [14].

Figure 2: Determination of w_g' in a sucrose-water mixture using the intercept of the experimental evaluated T_m peaks (squares) fitted with the Chen model corresponding to Equation (1) and the onset of the corresponding T_g' (dots) fitted as horizontal line.

Figure 3: Exemplary DSC trace of 62% sucrose with ΔH integrated starting from the onset of T_g' until the end of the melting event.

Figure 4: Determination of w_g' in a sucrose-water mixture using the change in melting enthalpy.

Figure 5: A: Frozen water content obtained from the melting enthalpy in a sucrose-water mixture and B: calculated w_g' thereof.

Figure 6: w_g' results of different sugar based systems with varied mAb concentrations.

Figure 7: Exemplary DSC thermogram of 19% mAb in HPW. Estimation of T_g' onset is depicted in the zoom. The onset of T_g' at about -25°C was used as starting point for the integration of the melting event.

Table 1

Abbreviation	Formulation	Sugar	Buffer	Further excipient	mAb
Suc	Sucrose	7	--	--	0, 0.2, 1, 5, 20
Suc+His 5.3	Sucrose + Histidine pH 5.3	7	0.23	--	0, 0.2, 1
Suc+His 7.4	Sucrose + Histidine pH 7.4	7	0.23	--	0, 0.2, 1
Suc+Phos 5.3	Sucrose + Phosphate pH 5.3	7	0.15	--	0, 0.2, 1
Suc+Phos 7.4	Sucrose + Phosphate pH 7.4	7	0.15	--	0, 0.2, 1
Suc+0.4NaCl	Sucrose + NaCl	7	--	0.4	0, 0.2, 1
Suc+0.8NaCl	Sucrose + NaCl	7	--	0.8	0, 0.2, 1
Tre	Trehalose	7	--	--	0, 0.2, 1, 10
ArgCitr	Arginine citrate	--	--	5	--
ArgHCl	Arginine*HCl	--	--	5	0, 0.2
NaCl	NaCl	--	--	0.4	1
mAb	mAb	--	--	--	<i>pure</i>

Table 2

w_g' [%]	Starting liquid				Freeze concentrate			
	Sucrose [%]	Histidine buffer [%]	mAb [%]	H ₂ O [%]	Sucrose [%]	Histidine buffer [%]	mAb [%]	H ₂ O [%]
74.3	7	--	0.2	92.8	72.2	--	2.1	25.7
72.4	7	0.23	1	92.0	61.6	2.0	8.8	27.6
78.0	7	--	20	73.0	20.2	--	57.8	22.0

Figure 1

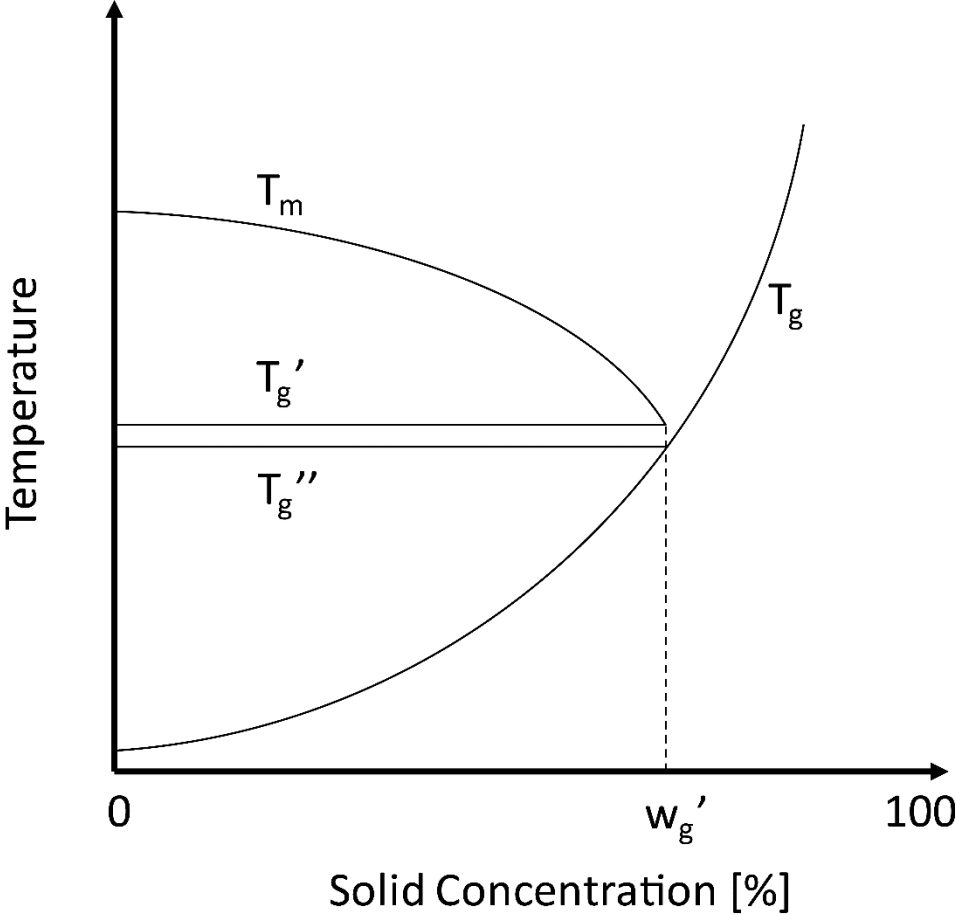


Figure 2

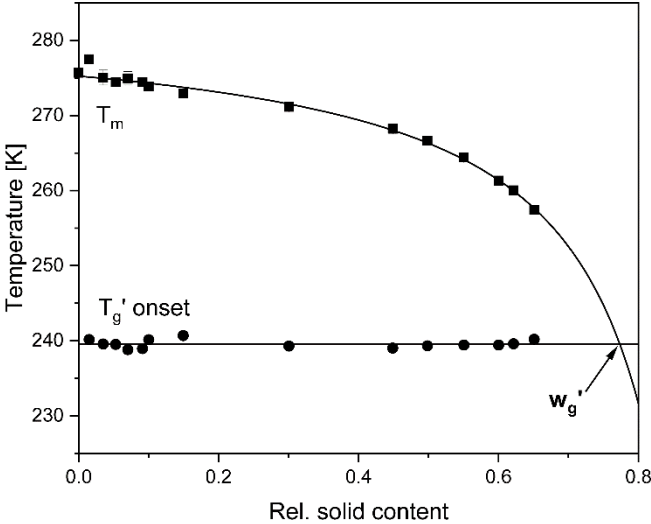


Figure 3

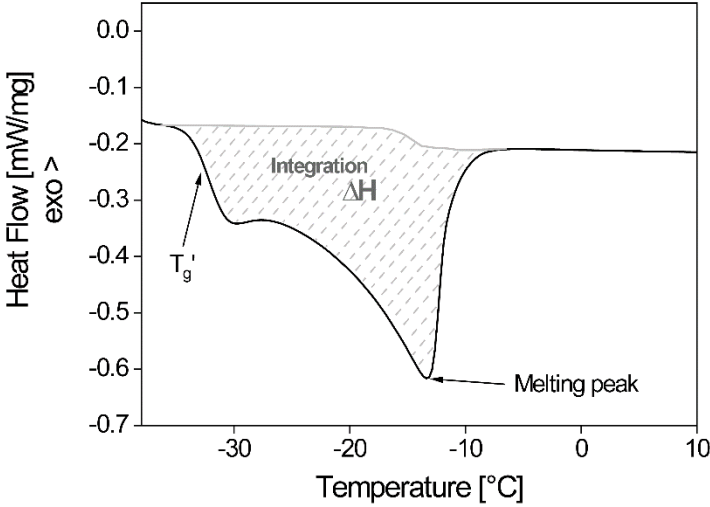


Figure 4

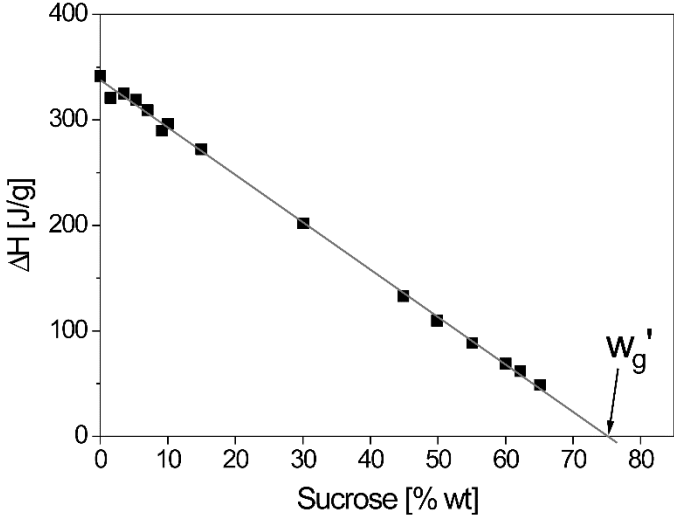


Figure 5

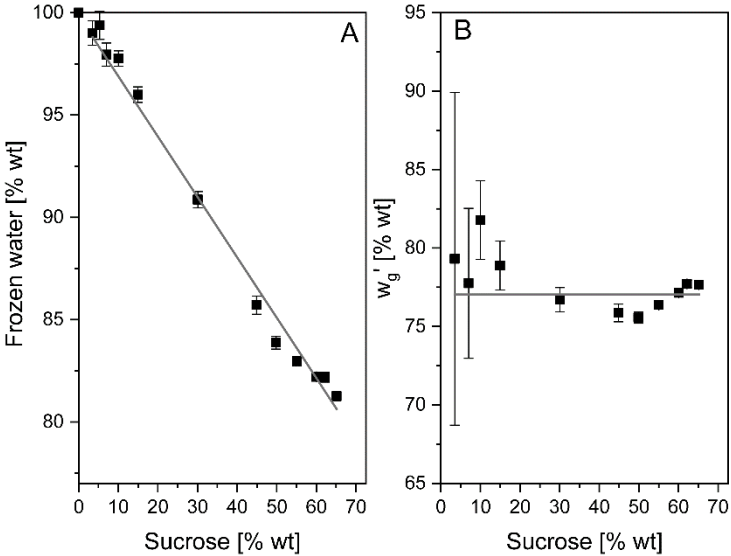


Figure 6

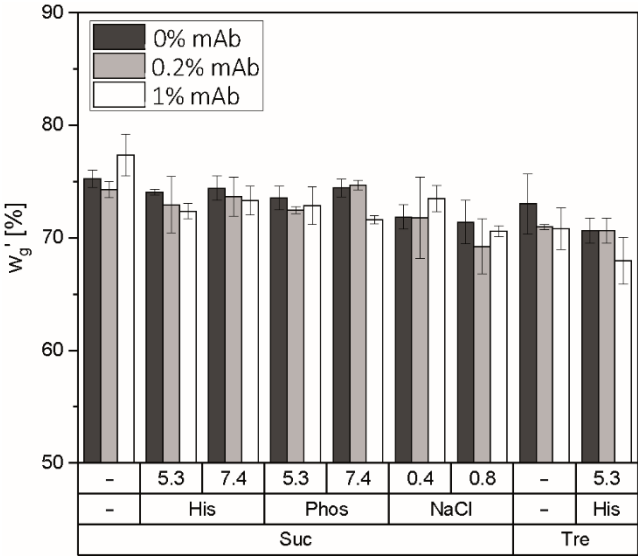
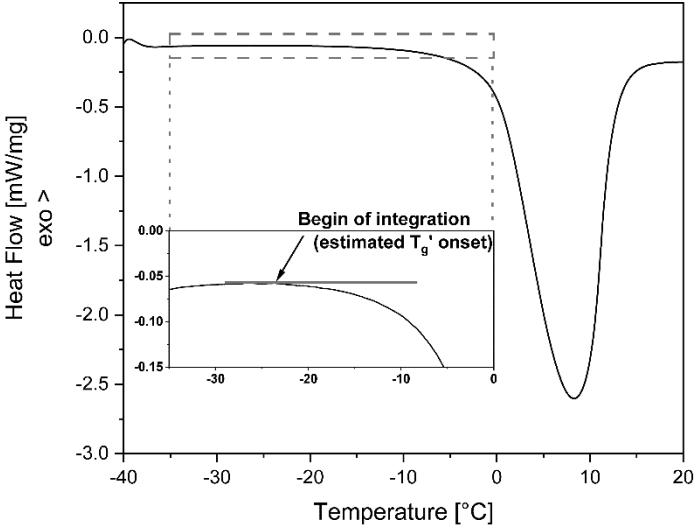


Figure 7



Supplement

